Materials Research Bulletin 83 (2016) 128–134

Contents lists available at ScienceDirect

Materials Research Bulletin

journal homepage: www.elsevier.com/locate/matresbu

Effect of substitutional As impurity on electrical and optical properties of β-Si_3N_4 structure

E. Kutlu[a,*], P. Narin[a], G. Atmaca[a], B. Sarikavak-Lisesivdin[a], S.B. Lisesivdin[a], E. Özbay[b,c,d]

[a] Department of Physics, Faculty of Science, Gazi University, Teknikokullar, 06500 Ankara, Turkey
[b] Nanotechnology Research Center, Bilkent University, Bilkent, 06800 Ankara, Turkey
[c] Department of Physics, Bilkent University, Bilkent, 06800 Ankara, Turkey
[d] Department of Electrical and Electronics Engineering, Bilkent University, Bilkent, 06800 Ankara, Turkey

ARTICLE INFO

Article history:
Received 28 September 2015
Received in revised form 13 May 2016
Accepted 15 May 2016
Available online 17 May 2016

Keywords:
A. Electronic materials
A. Optical materials
B. Optical properties
D. Dielectric properties
D. Electrical properties

ABSTRACT

β-Si_3N_4 is used as the gate dielectric for surface passivation in GaN-based, high-electron mobility transistors(HEMTs). In this study, the electrical and optical characteristics of the hexagonal β-Si_3N_4 crystal structure were calculated using density functional theory (DFT) and local-density approximation (LDA). Calculations of the electronic band structure and the density of states (DOS) were made for the pure β-Si_3N_4 crystal structure and the β-Si_3N_4 crystal doped with an arsenic (As) impurity atom. In addition, the optical properties such as the static dielectric constant, refractive index, extinction coefficient, absorption coefficient and reflection coefficient were examined depending on the photon energy. As a result of these calculations, it was observed that the As impurity atom drastically changed the electrical and optical properties of the pure β-Si_3N_4 crystalline structure, and improvements are suggested for potential further studies.

1. Introduction

Pure β-Si_3N_4 crystals are frequently used in electronic and thermal applications since they have a high forbidden band-gap, strong mechanical properties and an ability to operate at high temperatures [1,2]. Si_3N_4 is an important dielectric material used for the surface passivation of the structures in transistor and light-emitting diode (LED) applications and in gate dielectric applications [3]. The β-Si_3N_4 material is suitable to be used in GaN-based structures because of the hexagonal structure of this dielectric material, which is similar to the hexagonal structure of GaN.

β-Si_3N_4 is a crystalline structure which has six silicon and eight nitrogen atoms in a fourteen-atom unit cell in the $P6_3/m$ space group. Si_3N_4 can also be found in nature in cubic (γ) and trigonal (α) crystal structures [4]. Depending on the different stoichiometric properties, the silicon (Si) and nitrogen (N) ratios can vary [5].

Today, β-Si_3N_4 crystals can be grown as quality crystal structures using the *in-situ* chemical vapor deposition (CVD) and molecular beam epitaxial (MBE) methods [6–8]. In the growth process, when using MBE for growth in particular, the impurity atoms in the medium penetrate the growing crystal and this changes the electrical and optical properties of the crystal considerably [9]. For example, in reactors in which As is used for crystal growth, the potential As impurity in the medium can be found in every growth of Si_3N_4 which is performed in the related reactor. In reactors in which As is used, growth takes place under As_2 vapor and this results in the entire interior surface of growth chamber being covered by arsenic. For this reason, the impact of the possible As impurity in the β-Si_3N_4 material on the electrical and optical properties of β-Si_3N_4 forms the basis of this study.

2. Calculation method

In this study, Atomistix Toolkit-Visual NanoLab (ATK-VNL) software was used to perform the calculations [10–12]. The cut-off energy and k-points were set to 280 eV and $4 \times 4 \times 10$ respectively in order to analyse the electrical and optical properties of β-Si_3N_4. For the studied structure, the optimized lattice constants were found to be a = 7.6015 Å, c = 2.9061 Å as shown in Table 1. The lattice constants which were used in the calculations were almost compatible with the experimental lattice constants [13,14]. Also, the local density approximation (LDA) approach was used for the exchange-correlation. Because the LDA approach gives very good results in terms of the electronic properties of the investigated structure, the calculations of the optical properties were also made

* Corresponding author.
E-mail address: eciss06@gmail.com (E. Kutlu).

http://dx.doi.org/10.1016/j.materresbull.2016.05.017
0025-5408/

Table 1
For β-Si_3N_4, lattice parameters of both present study and experimental studies.

β-Si_3N_4	Present study [20]	Experimental 1 [13]	Experimental 2 [14]
a (Å)	7.601	7.608	7.586
c (Å)	2.906	2.891	2.902
c/a	0.382	3.799	0.382

using this approach. In the calculations, the maximum force applied to the crystal was 0.05 eV/Å.

The energy range of 0–15 eV was chosen for the calculation of the optical properties. The electrical and optical properties were calculated for the pure β-Si_3N_4 crystal. All possible Si- and N-sites were used for the As impurity atom to determine the most stable structure as discussed later in this study, and subsequent electrical and optical properties for the most stable structure were calculated in sequence.

3. Results and discussion

3.1. Electronic properties

To determine the most probable position of the As impurity in the lattice, the binding energies and the formation energies of the related structures were calculated with the help of Eqs. (1) and (2) respectively. In Eq. (1), E_b, E_{tot} and E_{atoms} were the binding energy, the total energy of the structure and the sums of the total energy of each atom of the structure respectively. The stability of the structure is related to the value of the binding energy of the system [15–18]. In Eq. (2), E_F, E_{tot}^{doped}, E_{tot}^{pure}, μ_{imp} and μ_{sub} represent the formation energy, the total energy of the structure with As impurity, the total energy of the pure structure, the chemical potential of the impurity atom and the chemical potential N or Si atoms which constituted the unit cell respectively [19]. The chemical potential value of Si was taken from the total energy per atom of the bulk Si. The chemical potential values of As and N were determined as the energy of the As_2 and N_2 molecules ($\mu_{As} = 1/2\,\mu(As_2)$ and $\mu_N = 1/2\,\mu(N_2)$). The binding energies, formation energies and total energy per atom values are listed for each atomic position of the structure in Table 2. The atomic positions are named in Fig. 1. The most probable impurity positions were found to be in positions 3 and 4, which were Si-sites, because they had the lowest total energies, formation energies and binding energies. Similar energy values can be found in the literature [21]. Further calculations of the investigated structure with As impurity in this study were made for the As impurity atom at position 3, which is shown by the red circle in Fig. 1.

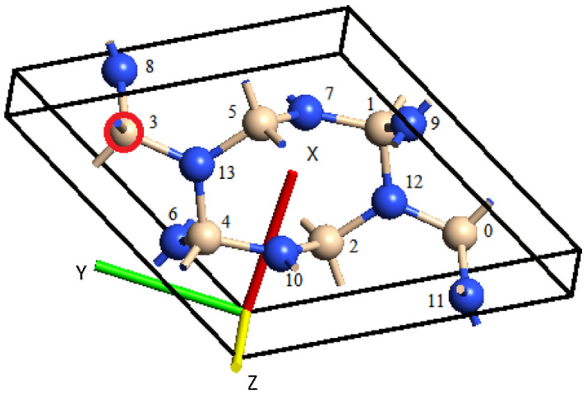

Fig. 1. 14-atom unit cell of pure β-Si_3N_4. Yellow and blue spheres represent silicon and nitrogen, respectively. Red circle represent the most stable atomic position for As impurity. (For interpretation of the references to color in this figure legend, the reader is referred to the web version of this article.)

$$E_b = E_{tot} - E_{atoms} \tag{1}$$

$$E_F = E_{tot}^{doped} - [E_{tot}^{pure} + \mu_{imp} - \mu_{sub}] \tag{2}$$

Fig. 2 shows the total energy per atom, which depends on the individual variation of the lattice constants. The lowest total energy value per one atom was found to be $E_{tot} = -234.09$ eV. This value was the most stable state when the lattice constants were a = 7.6015 Å and c = 2.9061 Å [20].

The band structures and density of states (DOS) of the β-Si_3N_4 with and without As impurity are shown in Fig. 3(a) and (b) respectively. The band structures have indirect characteristics. As shown in Fig. 3(a), the band-gap of the pure β-Si_3N_4 was found to be ~4.95 eV, which was in agreement with the experimental values. The experimental band-gap can be found to be between 4.5 and 5.5 eV in the literature [22,23]. An impurity band in the vicinity of the Fermi level was found for the structure with As impurity. The source of the charges which formed this impurity band came from the hybridization of the p shell of the arsenic atom and the s shell of the nitrogen atom. This resulting impurity band degraded the electrical properties of the β-Si_3N_4, which is an insulator material in its pure form. Also, on the DOS graph, an extended peak just above the Fermi level was observed. The DOS peak related to the impurity band had a significant DOS density with respect to the conduction band.

Table 2
Total Energy per atom, Formation Energy and Binding Energy values for the structure with the As impurity place in the situations where the As impurity is replaced with the given atom shown in Fig. 1.

Atom #	Atoms	Total Energy Per Atom (eV)	Formation Energy (eV)	Binding Energy (eV)
0	Silicon	−243.80147	8.06974	−102.8348
1	Silicon	−243.80111	8.07478	−102.8297
2	Silicon	−243.80110	8.0749	−102.8296
3	***Silicon***	***−244.02119***	***4.99368***	***−105.9108***
4	***Silicon***	***−244.02116***	***4.99412***	***−105.9104***
5	Silicon	−243.13233	17.43767	−93.4669
6	Nitrogen	−237.36595	10.94232	−99.9622
7	Nitrogen	−237.34098	11.29184	−99.6127
8	Nitrogen	−237.14300	14.06353	−96.8410
9	Nitrogen	−237.31433	11.66492	−99.2396
10	Nitrogen	−237.49824	9.09017	−101.8144
11	Nitrogen	−237.18700	13.44761	−97.4569
12	Nitrogen	−237.19109	13.39032	−97.5142
13	Nitrogen	−237.19109	13.39032	−97.5142

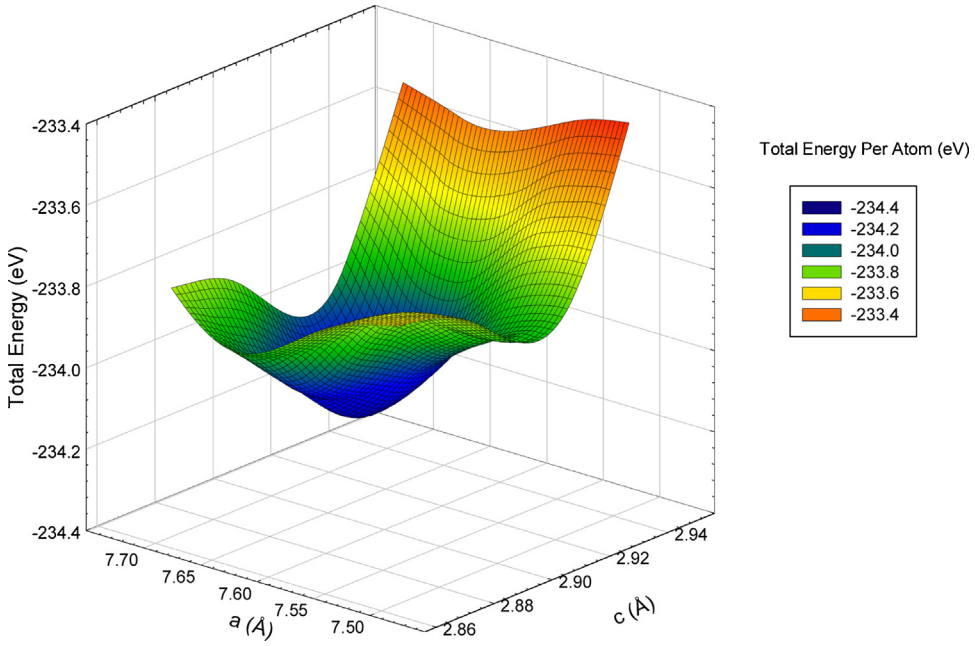

Fig. 2. The total energy plot per atom, depending on the lattice constants.

3.2. Optical properties

Analyses of the optical properties of the pure β-Si_3N_4 and the β-Si_3N_4 doped with As impurity structures were carried out in the range of 0–15 eV. The complex structure of the dielectric function is given by the well-known Eq. (3) [24].

$$\varepsilon(\omega) = \varepsilon_1(\omega) + i\varepsilon_2(\omega), \tag{3}$$

where,

$$\varepsilon_1(\omega) = 1 + \frac{2}{\pi} P \int_0^{\infty} \frac{\omega' \varepsilon_2(\omega')}{\omega'^2 - \omega^2} d\omega' \tag{4}$$

$$\varepsilon_2(\omega) = \frac{e_2 h}{\pi m^2 \omega^2} \sum \sum \int |eP_{if}|^2 \delta(E_f^K - E_i^K - \hbar\omega) d^3k \tag{5}$$

The real and imaginary parts of the dielectric function are given by the Kramers-Kronig equations in the Eqs. (4) and (5) respectively [25]. The frequency-dependent $\varepsilon_1(\omega)$ functions for the β-Si_3N_4 structures doped with and without As impurity are given in Fig. 4. The structure featured anisotropic optical properties as a result of its wurtzite crystal structure. Significant differences in optical properties were observed along the z-axis [0001] growth direction. In the pure structure, $\varepsilon_1^{xx}(\omega)$ and $\varepsilon_1^{yy}(\omega)$were found to be isotropic as expected. In the structure with As impurity, the impurity was found to induce a slight anisotropy between $\varepsilon_1^{xx}(\omega)$and $\varepsilon_1^{yy}(\omega)$. In the pure β-$Si_3N_4$ structure, the static dielectric constant was found to be ~5.52. Depending on the increasing photon energy, an increase in $\varepsilon_1(\omega)$ values was observed in the range of 0–7 eV. Despite the increase in the energy, a decrease in the value of $\varepsilon_1(\omega)$ was observed in the range 7–15 eV.

The relation between the absorption coefficient and the dielectric constant is given in Eq. (6) [26].

$$\varepsilon_1 = n^2 - k^2 \tag{6}$$

Here, n and k are the refractive index and the extinction coefficient respectively. In Eq. (10), the extinction and the absorption coefficients can be seen to be associated with each other directly. With increasing the photon energy, the absorption coefficient increases and depending on Eq. (10) the extinction coefficient value also increases. As a result, as Figs. 4(a) and 9(a) show, especially after the 7 eV, the dielectric constant decreases with respect to Eq. (6). The energy value of the first peak of $\varepsilon_1(\omega)$ was ~6.8 eV, and the dielectric constant at this frequency was 14.9. It can be said that the structure exhibited a metallic behavior at the points where the real part of the dielectric function fell below zero, and the structure exhibited a dielectric behavior above zero.

The static dielectric constant in the dielectric function for the structure with the As impurity was calculated as 6.55. The first peak value of $\varepsilon_1(\omega)$ was at 1.79 eV. The highest dielectric coefficient was 10.88 at 6.9 eV.

Fig. 5 shows the frequency-dependent $\varepsilon_2(\omega)$ functions for the β-Si_3N_4 structures doped with and without As impurity. In the pure structure, $\varepsilon_2^{xx}(\omega)$ and $\varepsilon_2^{yy}(\omega)$were found to be almost isotropic as was also found for the $\varepsilon_1(\omega)$ functions. Similarly, in the structure with As impurity, the impurity was found to induce a slight anisotropy between $\varepsilon_2^{xx}(\omega)$and $\varepsilon_2^{yy}(\omega)$. In both graphs, the starting point of the peak gives the optical band-gap where the optical transitions take place. The optical band-gap value for the pure β-Si_3N_4 was found to be in the range of ~5–5.8 eV which is in agreement with the literature [27–29]. The energy values where the optical transitions were at maximum were found to be 7.2 eV and 9 eV. The optical band-gap value for the structure with As impurity was found to be in the range of ~1–1.3 eV, which was caused by states induced at the middle of the band-gap of the related pure structure. Again, for this structure, high peak values were observed at ~2 eV and in the range of 7.5–9 eV. These regions indicate the points where absorption was high for the β-Si_3N_4 structure doped with As impurity.

The real and imaginary parts of the refractive index, the reflectivity and the absorption coefficient for the crystal structures respectively are given by the following equations as [30,31];

$$n(\omega) = (1/\sqrt{2}) \left[\sqrt{\varepsilon_1^2(\omega) + \varepsilon_2^2(\omega)} + \varepsilon_1(\omega) \right]^{1/2}, \tag{7}$$

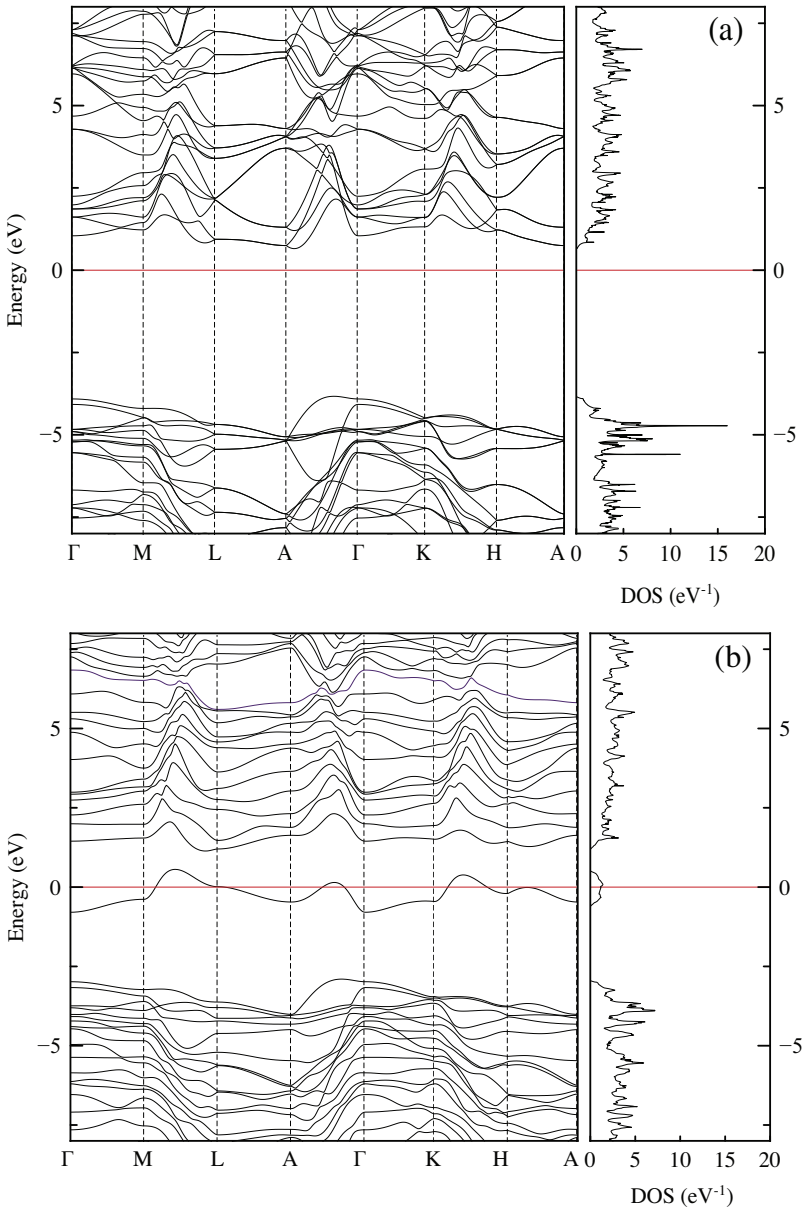

Fig. 3. Band structures and density of states, (a) pure β-Si_3N_4, (b) β-Si_3N_4 doped with As impurity.

$$k(\omega) = (1/\sqrt{2})\left[\sqrt{\varepsilon_2^1(\omega) + \varepsilon_2^2(\omega)} - \varepsilon_1(\omega)\right]^{1/2},$$

$$R(\omega) = \frac{(n-1)^2 + k^2}{(n+1)^2 + k^2}, \tag{9}$$

$$\alpha(\omega) = 2\frac{\omega}{c}k. \tag{10}$$

Fig. 6(a) shows the frequency-dependent change in the real part of refractive index of the pure β-Si_3N_4. The refractive index is given as Eq. (7).

If $\varepsilon_1(\omega) >> \varepsilon_2(\omega)$, which is true in Fig. 5(a) up to 6 eV, the refractive index turns into Eq. (11)

$$n(\omega) \cong \sqrt{\varepsilon_1(\omega)} \tag{11}$$

For this reason, at the low energy part of Fig. 4(a), the refractive index is determined by the real part of the dielectric function.

If $\varepsilon_2(\omega) >> \varepsilon_1(\omega)$, the refractive index turns into Eq. (12)

$$n(\omega) \cong \sqrt{\frac{\varepsilon_2(\omega)}{2}} \tag{12}$$

The refractive index was therefore determined by the imaginary part of the dielectric function at the related parts of Figs. 4(a) and 5(a). In the other energy values, the refractive index was defined with both $\varepsilon_1(\omega)$ and $\varepsilon_2(\omega)$. Here, a high refractive index was observed at higher wavelengths and there was a normal dispersion in the range of 0–7 eV. In the literature, the refractive index for a pure β-Si_3N_4 structure was given as being between 1.99 and 2.04

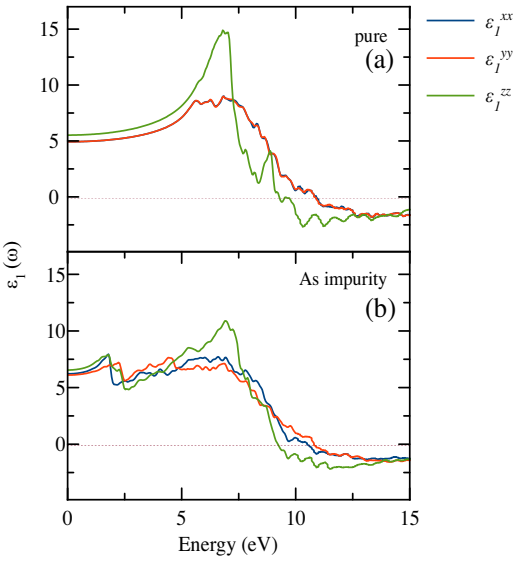

Fig. 4. The changes in the real part of the dielectric function depending on the frequency for (a) pure β-Si_3N_4 crystal, and (b) for β-Si_3N_4 crystal doped with As impurity.

[32,33]. We found in our study that the refractive index constant was $n(0) = 2.35$: the highest refractive index value was found to be 4.15 at an energy level of 7.1 eV.

Fig. 6(b) shows that the β-Si_3N_4 doped with As impurity had a higher refractive index at higher wavelengths. The refractive index constant was found to be $n(0) = 2.56$. The maximum value of the refractive index was found to be 3.48 at approximately 7 eV.

Fig. 7 shows the frequency-dependent change in the imaginary part of the refractive index for the pure β-Si_3N_4 structure and the β-Si_3N_4 structure doped with As impurity. The imaginary part of the refractive index is related to absorption. The areas of the high imaginary part of the refractive index possess a high absorption capacity.

The energy levels in the range of 4.9–15 eV for the pure β-Si_3N_4 crystal and the energy levels in the range of 1.2–2.5 eV, 5–15 eV for the crystal doped with As impurity indicate the high absorption areas.

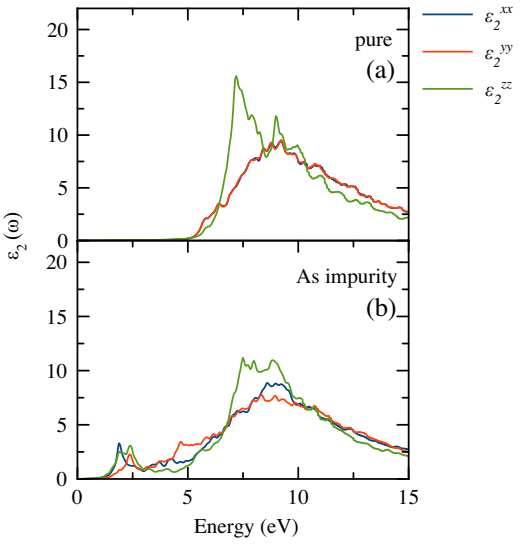

Fig. 5. The changes in the imaginary part of the dielectric function depending on the frequency for (a) pure β-Si_3N_4 crystal, and (b) for β-Si_3N_4 crystal doped with As impurity.

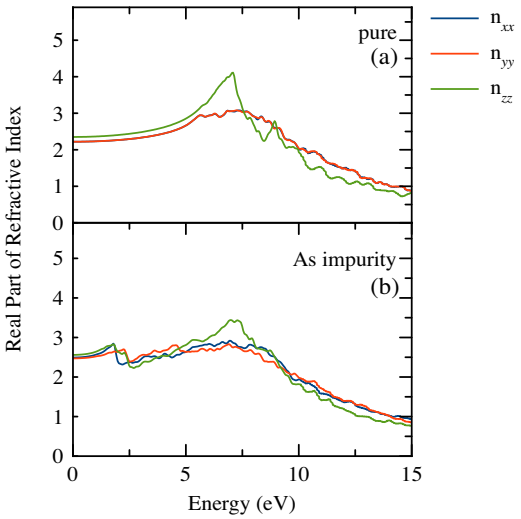

Fig. 6. The real part of the refractive index for (a) pure β-Si_3N_4, (b) β-Si_3N_4 doped with As impurity.

Fig. 8 presents the frequency-dependent change in the reflectivity of the pure structure and the structure doped with As impurity. A high anisotropic change was observed along the z-axis of the pure β-Si_3N_4 crystal. The reflectivity values show a partly isotropic change for both crystals but especially for the structure doped with As impurity. It can be seen that the reflectivity was high, in the range of 0–10 eV, compared with other levels. The reflection coefficients of the pure structure and the structure doped with As impurity were found to be 0.16 and 0.19 respectively.

Fig. 9 shows the frequency-dependent change in the absorption coefficients of the pure β-Si_3N_4 and the β-Si_3N_4 doped with As impurity. The absorption regions of the pure structure and the structure doped with As impurity start at energy levels of ~5 eV and ~1.2 eV respectively. It can be observed that there was no absorption at higher wavelengths and that the absorption increased as the wavelength decreased. Similar to the reflectivity, As impurity induces an isotropy in the absorption when the pure structure shows a high anisotropy in the z-axis.

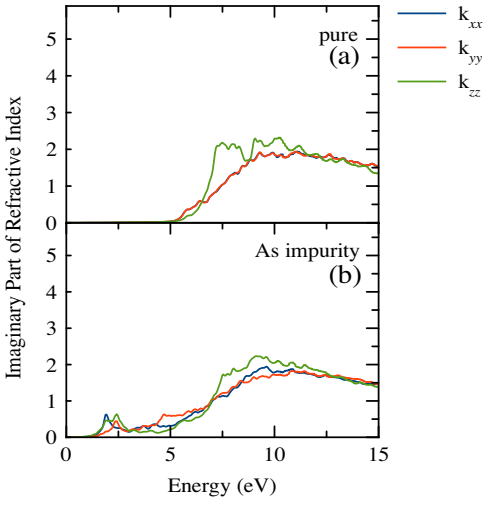

Fig. 7. The imaginary part of the refractive index for (a) pure β-Si_3N_4, (b) β-Si_3N_4 doped with As impurity.

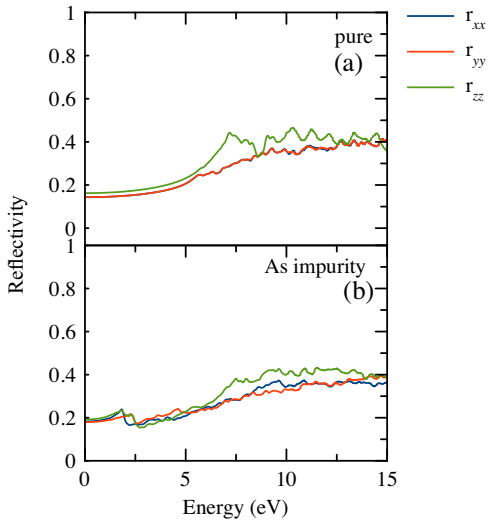

Fig. 8. Reflectivity for (a) pure β-Si_3N_4 crystal, (b) β-Si_3N_4 crystal doped with As impurity.

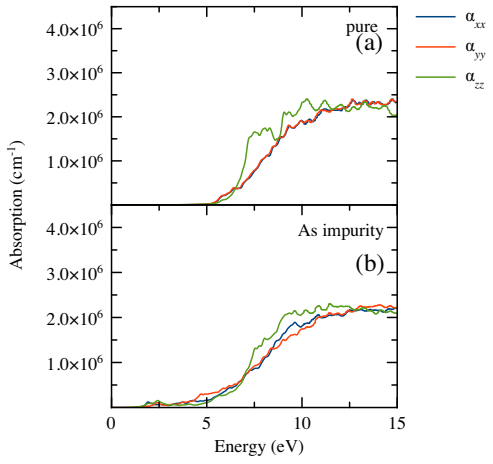

Fig. 9. The absorption coefficient for (a) pure β-Si_3N_4 crystal, (b) β-Si_3N_4 crystal doped with As impurity.

4. Conclusion

In this study, the electrical and optical properties of the pure β-Si_3N_4 structure and a structure doped with As impurity were investigated by DFT calculations using the LDA approach. The most stable state was calculated by the formation energy and binding energy approach when the As impurity atom was replaced by each atom in the unit cell of the investigated structure. In this way, the potential place of the As impurity atom was determined. In addition to this, the change in the total energy per atom, caused by the independent changes in the lattice constants, was examined. The impact of the As impurity atom on the band structure was analysed by comparing the band structures and it was found that As impurity induced an important deep level which was in the vicinity of the Fermi level. The optical properties of the pure β-Si_3N_4 structure and the structure obtained by placing the As atom in place of the atom with the least energy were analysed on the basis of the dielectric functions. Calculations of optical properties such as the real and imaginary parts of the refractive index, the reflection coefficient and the absorption coefficient were made for both cases. The optical constants were determined to be at zero frequency, and the changes in optical properties at higher frequencies were also examined. It was found that As impurity induced slight anisotropy in the real and the imaginary parts of dielectric functions and therefore the refractive indexes in x-axis and y-axis, which normally present isotropic behavior in the pure β-Si_3N_4 structure. Unlike the dielectric functions and the refractive indexes, As impurity induced an isotropy in the reflectivity and absorption when the pure structure showed high anisotropy in the z-axis.

Acknowledgements

This work is supported by the projects DPT-HAMIT, DPT-FOTON, NATO-SET-193 and TUBITAK under project nos. 113F364, 113E331, 109A015, and 109E301. One of the authors (E.O.) also acknowledges partial support from the Turkish Academy of Sciences.

References

[1] J.L. Iskoe, F.F. Lange, E.S. Diaz, Effect of selected impurities on the high temperature mechanical properties of hot-pressed silicon nitride, J. Mater. Sci. 11 (1976) 908–912.
[2] A.Y. Liu, M.L. Cohen, Structural properties and electronic structure of low-compressibility materials: β-Si_3N_4 and hypothetical β-C_3N_4, Phys. Rev. B 41 (1990) 10727–10734.
[3] X. Hu, A. Koudymov, G. Simin, J. Yang, M. Asif Khan, A. Tarakji, M.S. Shur, R. Gaska, Si_3N_4/AlGaN/GaN–metal–insulator–semiconductor heterostructure field–effect transistors, Appl. Phys. Lett. 79 (2001) 2832–2834.
[4] R. Belkada, T. Shibayanagi, M. Naka, M. Kohyama, Ab initio calculations of the atomic and electronic structure of β-silicon nitride, J. Am. Ceram. Soc. 83 (2000) 2449–2454.
[5] F.L. Riley, Silicon nitride and related materials, J. Am. Ceram. Soc. 83 (2000) 245–265.
[6] A. Zado, J. Gerlach, D.J. As, Low interface trapped charge density in MBE in situ grown Si_3N_4 cubic GaN MIS structures, Semicond. Sci. Technol. 27 (035020) (2012) 1–7.
[7] V.M. Bermudez, F.K. Perkins, Preparation and properties of clean Si_3N_4 surfaces, Appl. Surf. Sci. 235 (4) (2004) 406–419.
[8] M.E. Lattemann, S.U. Nold, H. Leiste, H. Holleck, Investigation and characterisation of silicon nitride and silicon carbide thin films, Surf. Coat. Technol. 174 (2003) 365–369.
[9] L. Xuefeng, P. La, X. Guo, Y. Wei, X. Nan, L. He, Research of electronic structures and optical properties of Na- and Mg-doped β-Si_3N_4 based on the first-principles calculations, Comput. Mater. Sci. 79 (2013) 174–181.
[10] Version 12.2.2 QuantumWise A/S.<http://www.quantumwise.com>.
[11] M. Brandbyge, J.L. Mozos, P. Ordejón, J. Taylor, K. Stokbro, Density-functional method for nonequilibrium electron transport, Phys. Rev. B 65 (165401) (2002) 1–17.
[12] J.M. Soler, E. Artacho, J.D. Gale, A. Garcıá, J. Junquera, P. Ordejón, D. Sánchez-Portal, The SIESTA method for *ab initio* order-*N* materials simulation, J. Phys. Condens. Matter 14 (2002) 2745–2779.
[13] P. Villars, L.D. Calvert, W.B. Pearson, Pearson's Handbook of Crystallographic Data for Intermetallic Phases, vols. 1–3, ASM, 1985 3258.
[14] W.Y. Ching, Y.N. Xu, J.D. Gale, M. Rühle, Ab-initio total energy calculation of α-and β-silicon nitride and the derivation of effective pair potentials with application to lattice dynamics, J. Am. Ceram. Soc. 81 (12) (1998) 3189–3196.
[15] B. Sarikavak-Lisesivdin, S.B. Lisesivdin, E. Ozbay, Ab initio study of Ru-terminated and Ru-doped armchair graphene nanoribbons, Mol. Phys. 110 (18) (2012) 2295–2300.
[16] Y.C. Ding, A.P. Xiang, M. Xu, W.J. Zhu, Electronic structures and optical properties of γ-Si_3N_4 doped with La, Physica B 403 (13) (2008) 2200–2206.
[17] Y.C. Ding, A.P. Xiang, J. Luo, X.J. He, Q. Cai, X.F. Hu, First-principles study electronic and optical properties of p-type Al-doped γ-Si_3N_4, Physica B 405 (3) (2010) 828–833.
[18] X.F. Lu, D. Qiu, M. Chen, L. Fan, C. Wang, H.J. Wang, G.J. Qiao, First principles calculations of electronic structures and optical properties of Al-and Ca-doped β-Si_3N_4, Mater. Res. Innov. 17 (3) (2013) 201–206.
[19] Kesong Yang, Ying Dai, Baibiao Huang, Han. Shenghao, Theoretical study of N-doped TiO_2 rutile crystals, J. Phys. Chem. B110 (47) (2006) 24011–24014.
[20] D. Boulay, D. Nobuo Ishizawa, Tooru Atake, V. Streltsov, Kennji Furuya and Fumio Munakata. Synchrotron X-ray and ab initio studies of β-Si3N4, Acta Crystallogr. Sect. B Struct. Sci. 60 (4) (2004) 388–405.
[21] F. Oba, K. Tatsumi, H. Adachi, I. Tanaka, n-and p-type dopants for cubic silicon nitride, Appl. Phys. Lett. 78 (11) (2001) 1577–1579.
[22] A.V. Vishnyakov, et al., The charge transport mechanism in silicon nitride: multi-phonon trap ionization, Solid State Electron. 53 (3) (2009) 251–255.
[23] R. Kärcher, L. Ley, R.L. Johnson, Electronic structure of hydrogenated and unhydrogenated amorphous SiN_x ($0 \leq x \leq 1.6$) A photoemission study, Phys. Rev. B 30 (1984) 1896–1910.

[24] Du, Yujie, et al., Electronic structure and optical properties of zinc-blende GaN, Optik 123 (24) (2012) 2208–2212.
[25] F. Wooten, Optical Properties of Solids, Academic Press, New York, 1972.
[26] R. Das, S. Pandey, Comparison of optical properties of bulk and nano crystalline thin films of CdS using different precursors, IJMSCI (2011).
[27] J.F. Nye, Clarendon Press, Oxford, 1957, pp. 297.
[28] Yong-Nian Xu, W.Y. Ching, Electronic structure and optical properties of α and β phases of silicon nitride, silicon oxynitride, and with comparison to silicon dioxide, Phys. Rev. B 51 (1995) 17379.
[29] H. Kurata, M. Hirose, Y. Osaka, Wide optical-gap photoconductive a-Si_xN_{1-x}:H, Jpn. J. Appl. Phys. 20 (1981) L811.
[30] X. Yu, C. Li, Y. Ling, T.A. Tang, Q. Wu, J. Kong, First principles calculations of electronic and optical properties of Mo-doped rutile TiO_2, J. Alloys Compd. 507 (1) (2010) 33–37.
[31] Y. Shen, Z. Zhou, Structural, electronic, and optical properties of ferroelectric $KTa_{1/2}Nb_{1/2}O_3$ solid solutions, J. Appl. Phys. 103 (2008) 074113.
[32] A.L. Shabalov, M.S. Feldman, M.Z. Bashirov, Optical properties of SiNx films of variable composition, Phys. Status Solidi (b) 145 (1988) K71–K74.
[33] R.W. Knoll, C.H. Henager Jr., Optical and physical properties of sputtered Si:Al:O:N films, J. Mater. Res. 7 (1992) 1247–1252.